



Journal of Renewable Energies

Revue des Energies Renouvelables

journal home page : <https://revue.cder.dz/index.php/rer>

Investigation of monocrystalline silicon surface texturization by image processing program

Abdellah Trad khodja^{a,*}, Abdelkader Elamrani^a, Faouzi Kezzoula^a, Chahinez Nasraoui^a and Seif-Eddine Friha^a

^a *Research Center in Semiconductor Technology for Energetic (CRTSE), Development of Semiconductor Conversion Devices Division (DDCS), 02, Bd Frantz Fanon Algiers, BP N° 140, Algeria*

* *Corresponding author, E-mail address: abdhadj2014@gmail.com*

Tel.: + 213 671099908

Abstract

One of the main issues in the photovoltaic industry of silicon solar cells is the optical losses via reflection. To overcome this issue, texturization (chemical etching) remains the most commonly used method to produce a random pyramid structure to reduce reflection and thus increase photocurrent generation. Because of the anisotropic etching property of alkaline solution, square-based upright pyramids are formed, i.e., the difference in etching rates between (100) and (111) planes. In this paper, the following etching solutions were studied: 4/10, 6/6, and 10/4 (KOH weight percentage/IPA volume percentage). The optical, morphological, and electric characterizations using UV-Vis spectroscopy, electron scanning microscopy (SEM), and quasi-steady-state photoconductance (QSSPC) device are performed. Also, the standard weighted reflectance (SWR) was calculated. The pyramid size distribution generated using KOH-IPA solutions was investigated using an image processing program (ImageJ) via SEM images. The calculation of the height of the pyramids reveals that the typical pyramid size ranges from 3 to 9 μm , with large pyramids of small proportions. Furthermore, when the pyramids are distributed in a mixture of tiny and medium pyramids in precise proportions, the reflectivity is at its lowest, and as the number of large pyramids rises, the reflectivity increases.

Keywords: ImageJ, Potassium hydroxide, Pyramids, Silicon, Texturization

1. Introduction

Until now, silicon solar cells have continued to dominate the photovoltaic industry, particularly crystalline silicon cells [1] because of their features, which include low cost, ease of manufacture, and environmental friendliness. Naturally, the reflectance on planar silicon surfaces is high, which is an issue for photocurrent generation.

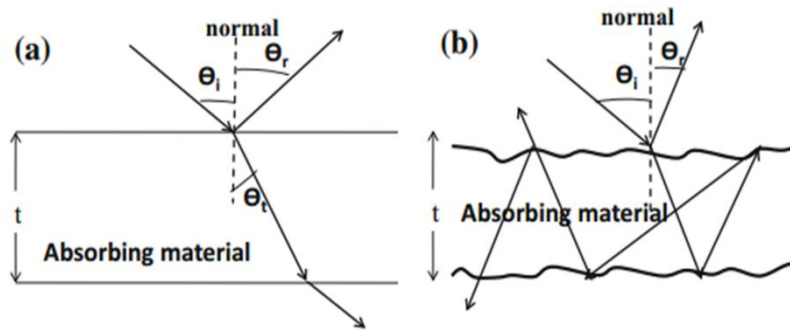


Fig 1. Schematic of light reflection, refraction and transmission on:
 a) planer surface b) rough surface

There are different methods to create structures to reduce total reflection on the silicon surface (Si). They are usually carried out through chemical etching [2, 3], mechanical grooving [4], laser grooving [5] or plasma etching [6]. In the monocrystalline silicon solar cell industry, the chemical etching method is the only one that allows a random pyramid structure. These structures have the advantage of decreasing the reflectance, resulting in improved light trapping and a subsequent higher photo conversion current in the solar cells. Several chemical baths can be used to generate these microstructures, such as $\text{Na}_2\text{CO}_3/\text{NaHCO}_3$ solutions [7-8], hydroxide (NaOH), isopropyl alcohol (IPA) [9], NH_4OH [10], and NaOCl [11]. The alkaline solutions operate anisotropically on crystalline silicon due to the difference in etching rates between the (100) and (111) planes. This etch shows randomly dispersed square-based upright pyramids on the surface (100) of the wafer, with faces corresponding to the (111) silicon wafer planes (figure 2) [12]. The link between the pyramids' height and base can be easily determined mathematically, where the value equals $\sqrt{2}/2$.

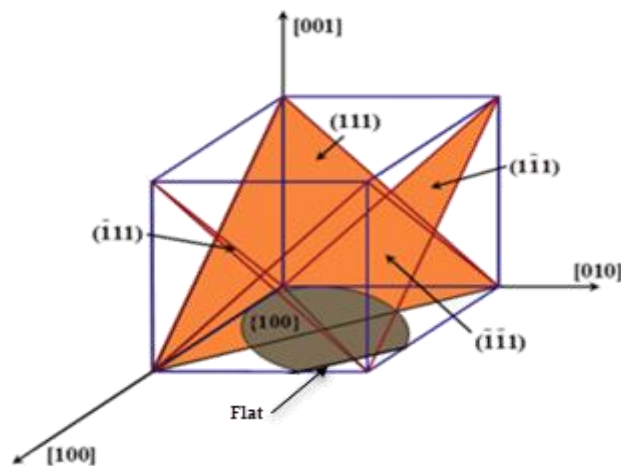


Fig 2. A diagram illustrating the origin of the pyramid structure: The planes (111) determine the pyramid's faces, and the plan (100) would be the base.

However, the etchant solution mixture of Potassium Hydroxide (KOH), and Isopropyl Alcohol (IPA), is commonly used as a standard process for industrial solar-cell texturization. The use of isopropyl alcohol (IPA) improves the wettability of the silicon surface and eliminates adherent hydrogen bubbles that attach to the silicon surface, resulting in improved random pyramid uniformity [6]. To maintain stability during the texturing process, IPA must be added to the solution frequently to keep it in the same concentration because of the evaporation of IPA. The etching process is illustrate in fig 3. Silicon interacts with potassium hydroxide and water to form potassium metasilicate and hydrogen as shown in the overall reaction equation below:

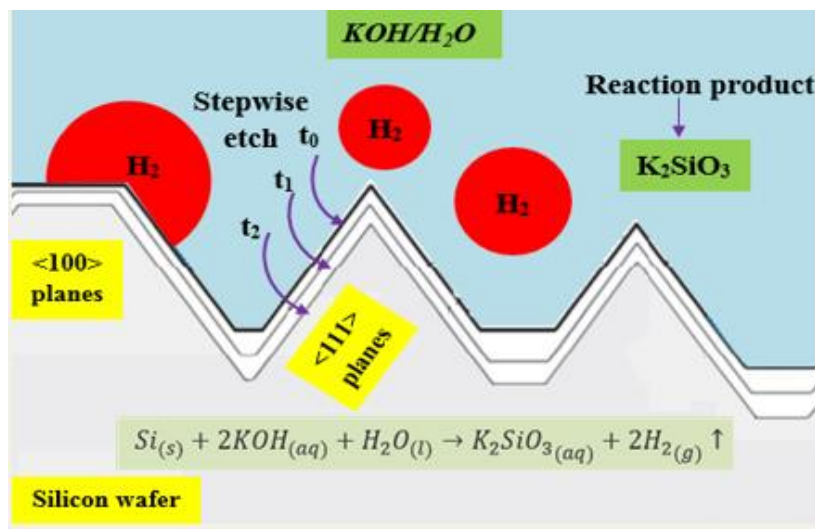
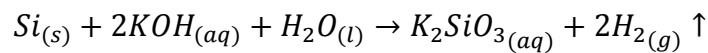


Fig 3. Schematic showing the silicon etch process

2. Experimental Section

In this work, n-type CZ wafers (100) oriented, 400 μm thick, and 2.8 $\Omega\cdot\text{cm}$ resistivity were used. The samples size were about two cm^2 . Before launching the etching process, the wafers were dipped in 2% HF for 1-2 min to remove native oxide, rinsed in running deionized water (DI-W), and afterward dried in blowing nitrogen gas. The following solutions were studied: 4/10, 6/6, and 10/4 (KOH wt.%/IPA vol.%). The samples were maintained in the solution for various etching times (20, 40, and 50 min), and the solution temperature was tuned to be around 80 $^\circ\text{C}$. Once the process of texturing was completed, the samples were rinsed in (DI-W) followed by 30% HCl (for 4 min) and 2% HF (for 1-2 min) to remove any metallic impurities or silicon oxide.

3. Results and discussion

The silicon samples' surface morphology was investigated using electron scanning microscopy (JSM-760Fplus). In order to quantify the optical performance, a UV-Vis spectrophotometer (CARY 500) was used to measure total surface reflectance in the wavelength range of 350 to 1200 nm. The electric characterization of minority charge carrier lifetime was carried out using a quasi-steady-state photoconductance (QSSPC) device (Sinton-WCT-120). To make a distinguished comparison of different textured specimens, the standard weighted reflectance (SWR) was calculated using the following formula [13]:

$$SWR_{\lambda_1 \rightarrow \lambda_2} = \frac{\int_{\lambda_1}^{\lambda_2} R(\lambda) S(\lambda) d\lambda}{\int_{\lambda_1}^{\lambda_2} S(\lambda) d\lambda}$$

Where $R(\lambda)$ is the calculated reflection, $S(\lambda)$ is the AM 1.5 sun spectrum for 350-1200 nm in 1 nm steps on each. The investigation of SEM images using the ImageJ program allowed us to determine the heights of the pyramids and their size distributions. Measurements of pyramid base edge lengths are provided automatically by this program. The heights of pyramids are calculated by dividing these lengths by 1.41 see Fig 4.

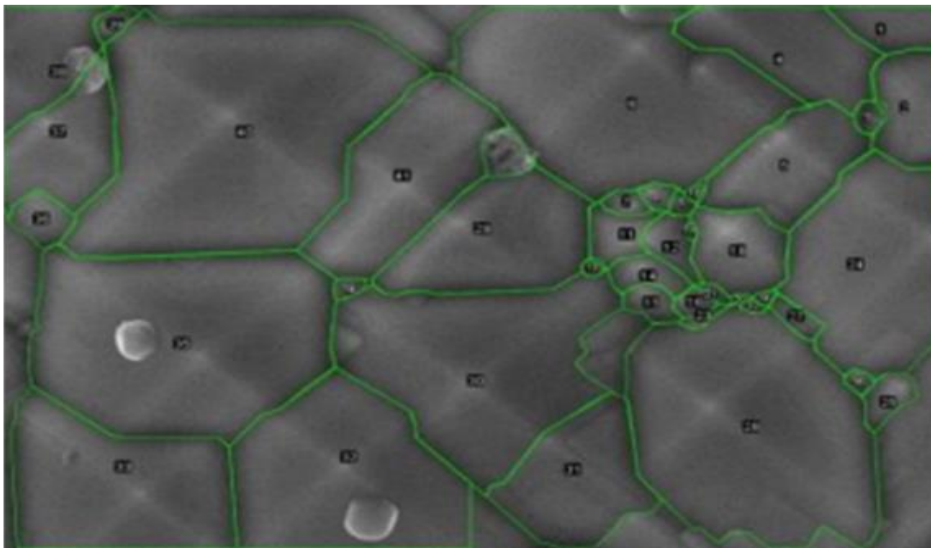


Fig 4. SEM image of textured surface analyzed by *ImageJ* program.

3.1 Optical analysis

Figure 5. depicts the reflectivity plot for the textured samples. According to Table 1, the sample with the lowest reflectance, 11.38%, was textured with a concentration of 6/6 (KOH wt. %/IPA vol. %), and process time of 20 min, whereas the sample with the highest reflectivity 14.08 %, was textured with a concentration of 10/4 (KOH wt. %/IPA vol. %) and process time of 50 min.

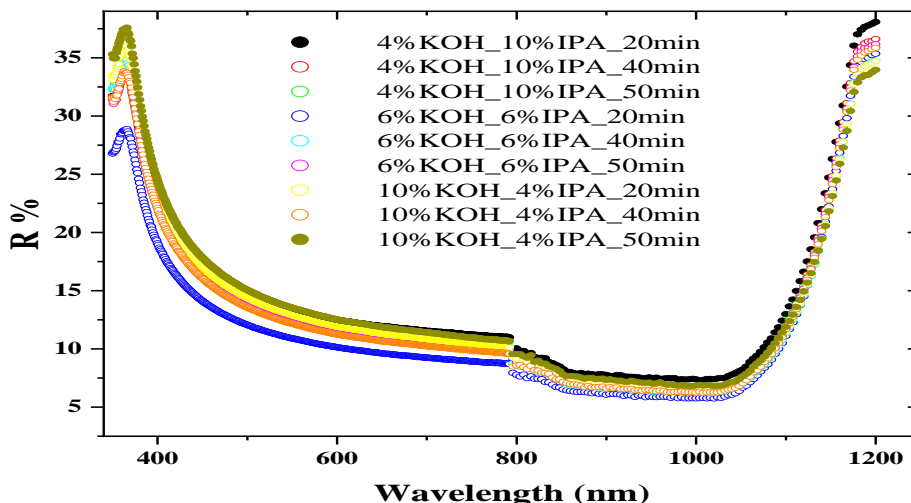


Fig 5. The reflectivity of textured samples.

Table 1. The calculated standard weighted reflectance (SWR) % for different concentrations and etching time

The solution concentration KOH wt.% / IPA vol.%	Etching time (min)		
	20	40	50
4/10	13.89 %	12.90 %	13.35 %
6/6	11.38 %	13.07 %	12.94 %
10/4	13.44 %	12.72 %	14.08 %

It was observed that for the process time (40 min), the reflectivity of the three solutions used did not differ significantly. Also, increasing the concentration of (IPA) by more than 6% increases the reflectivity; however, as time passes, the concentration of (IPA) decreases due to evaporation, resulting in a decrease in reflectivity (Fig 6).

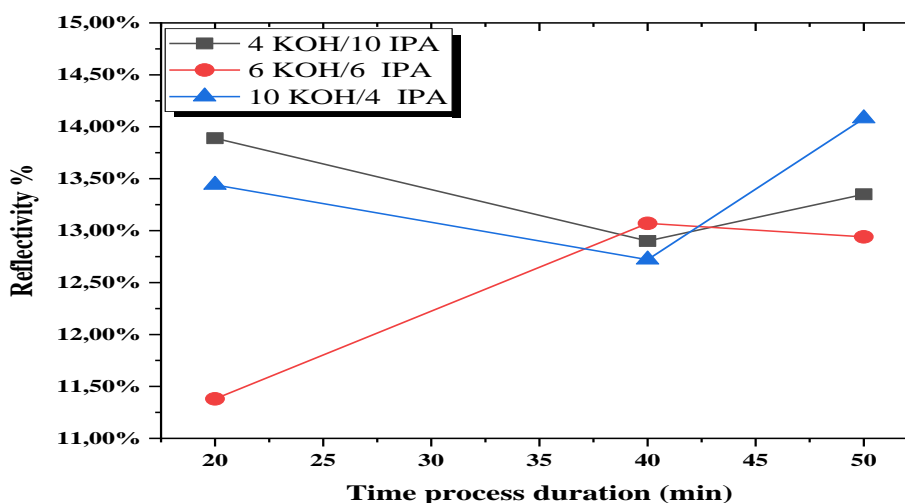


Fig 6. The reflectivity variation as a function of process time duration for the three solutions

3.2 Electrical analysis

Usually, lowering the optical reflectance of monocrystalline silicon solar cell enhances the minority carrier lifetime, and photoelectric conversion efficiency substantially. The effective minority carrier lifetime as a function of process time duration for the three solutions was determined and shown in Fig 6.

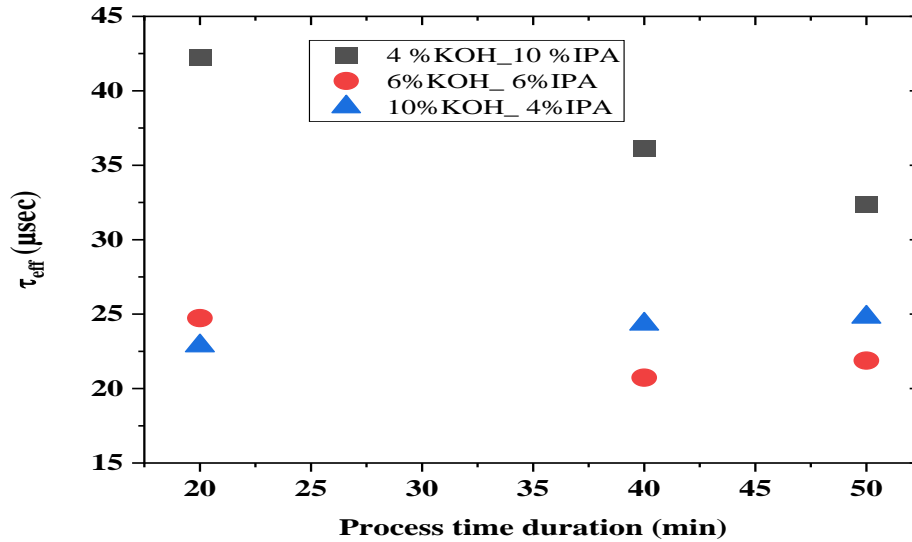


Fig 6. Effective minority carrier lifetime as a function of process time duration for the three solutions

According to the latter, it was found that there is no significant variation in effective minority carrier lifetime for both 4/10 and 6/6 (KOH wt. %/IPA vol. %) solutions. In contrast, the carrier lifetime of a 10/4 (KOH wt.%/IPA vol.%) solution decreases as the process duration increases. These variations were explained by the relationship between the density and the size of the pyramids.

3.3 Morphological analysis

The investigation of the surface morphology of the generated pyramids using KOH/IPA solutions was carried out by an image treating program (ImageJ) via SEM images.

It becomes clear from calculating the height of the pyramids that the average pyramid size varies from 3 μm to 9 μm with large pyramids in small proportions. In addition, when the distribution of the pyramids is a mixture of small and medium at specific proportions, the reflectivity is at its lowest value, and the increase of the large pyramids increases the reflectivity.

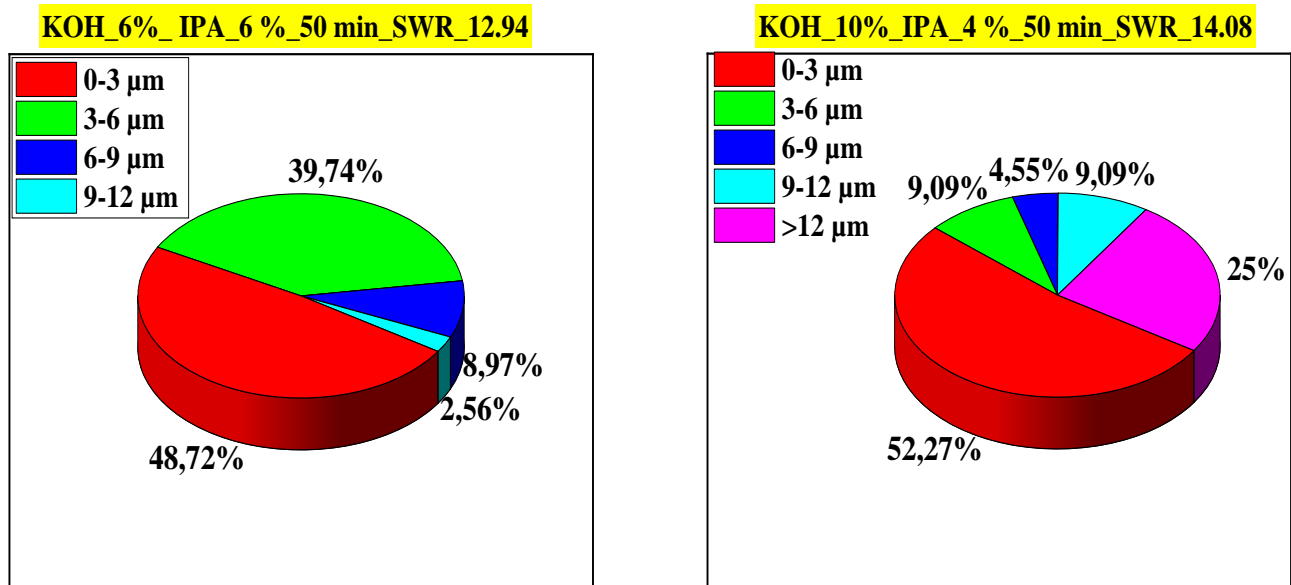


Fig 7. Pyramids size distributions for the lowest and the highest standard weighted reflectance

4. Conclusion

In this work, we investigated the pyramid size distribution generated using KOH-IPA solutions by an image processing program (ImageJ) via SEM images. The lowest SWR of 12.94 % is obtained for the solution 6/6 (KOH wt.%/IPA vol.%), 50 min process duration. The calculation of the height of the pyramids reveals that the typical pyramid size ranges from 3 to 9 μm , with large pyramids of small proportions. Furthermore, when the pyramids are distributed in a mixture of tiny and medium pyramids in precise proportions, the reflectivity is at its lowest, and as the number of large pyramids rises, the reflectivity increases.

5. Acknowledgements

The authors gratefully applaud Mrs. Saida Achacha for her cooperation in acquiring spectral measurements.

6. References

- [1] Sui, Muchen, et al. A review of technologies for high efficiency silicon solar cells. Journal of Physics: Conference Series 2021; 1907:012026-1. Doi:10.1088/1742-6596/1907/1/012026.
- [2] Palik, E. D., et al. Etching Roughness for (100), Silicon Surfaces in Aqueous KOH. Journal of Applied Physics 1991; 70:3291-6. doi.org/10.1063/1.349263.
- [3] Lee, Jaehyeong, et al. Optimization of Fabrication Process of High-Efficiency and Low-Cost Crystalline Silicon Solar Cell for Industrial Applications. Solar Energy Materials and Solar Cells 2009; 93:256-2. doi.org/10.1016/j.solmat.2008.10.013.

- [4] F. Restrepo and C. E. Backus. On black solar cells or the tetrahedral texturing of a silicon surface. *IEEE Trans. Electron Devices* 1976; 23:1195-10. doi
- [5] Verlinden, Pierre, et al. The Surface Texturization of Solar Cells: A New Method Using V-Grooves with Controllable Sidewall Angles. *Solar Energy Materials and Solar Cells* 1992; 26:71-1-2. doi.org/10.1016/0927-0248(92)90126-A.
- [6] S.R.Chitre, A high volume cost efficient production microstructuring process, in: *Proceedings of the 13th IEEE International Photovoltaic Specialist Conference, Washington DC, 1978*, pp. 152–154.
- [7] N. Marrero, B. González-Díaz, R. Guerrero-Lemus, D. Borchert, and C. Hernández-Rodríguez. Optimization of sodium carbonate texturization on large-area crystalline silicon solar cells. *Solar Energy Materials and Solar Cells* 2007;91:1943-20. doi.org/10.1016/j.solmat.2007.08.001.
- [8] A. Montesdeoca-Santana et al. XPS characterization of different thermal treatments in the ITO-Si interface of a carbonate-textured monocrystalline silicon solar cell. *Nucl. Instrum. Meth* 2010; 268:374-3-4. doi.org/10.1016/j.nimb.2009.09.044
- [9] E. Vazsonyi, K. De Clercq, R. Einhaus et al. Improved anisotropic etching process for industrial texturing of silicon solar cells. *Solar Energy Materials and Solar Cells* 1999; 57:179-26. doi.org/10.1016/S0927-0248 (98)00180-9
- [10] Silva A R, Miyoshi J, Diniz J A, et al. The Surface Texturing of Monocrystalline Silicon with NH₄OH and Ion Implantation for Applications in Solar Cells Compatible with CMOS Technology. *Energy Procedia* 2014, 44: 132. doi.org/10.1016/j.egypro.2013.12.019.
- [11] Basu PK, Sarangi D, Boreland MB. SingleComponent Damage-Etch Process for Improved Texturization of Monocrystalline Silicon Wafer Solar Cells. *IEEE J. Photovoltaics* 2013; 3:1222–8.
- [12] Zubel, I., Barycka, I. Silicon anisotropic etching in alkaline solutions I. The geometric description of figures developed under etching Si (100) in various solutions. *Sensors and Actuators A: Physical* 1998; 70:250-3. doi.org/10.1016/S0924-4247 (98)00141-1
- [13] Singh, Prashant, et al. Low Reflecting Hierarchically Textured Silicon by Silver Assisted Chemical Etching for Potential Solar Cell Application. *Materials Today: Proceedings* 2018; 5:23258- 11. doi.org/10.1016/j.matpr.2018.11.058.